All-electron and pseudopotential study of MgO: Equation of state, anharmonicity, and stability

Artem R. Oganov*
Department of Earth Sciences, University College London, Gower Street, London WC1E 6BT, United Kingdom

Peter I. Dorogokupets
Institute of the Earth's Crust, 128 Lermontov Street, 664033 Irkutsk, Russia

(Received 1 October 2002; revised manuscript received 6 February 2003; published 26 June 2003)

We have studied the high-pressure behavior of periclase (MgO) using density functional simulations within the generalized gradient approximation. The static and thermal (P-V-T) equation of state, B1-B2 transition pressure, elastic constants, Grüneisen parameter, and the intrinsic anharmonic parameters were calculated from static and *ab initio* molecular dynamics simulations. The simulations were performed using the projector augmented-wave and pseudopotential methods with different descriptions of the Mg atom (''small core'' and ''large core''). The errors of large-core pseudopotentials increase with pressure and are mainly due to the overlap between the Mg semicore (2p) orbitals and the valence orbitals, both of the same Mg atom and of the neighboring O atoms, rather than core deformation or core-core overlap effects. In agreement with previous works, we find that MgO remains in the B1 (''NaCl'') structure at all pressures existing within the Earth, and transforms into the CsCl-type structure at 509 GPa. Direct *ab initio* calculations avoid the simplifying assumptions inherent to many empirical treatments of thermoelasticity and allowed us to assess some of the common assumptions. We present a detailed qualitative analysis of the effects of intrinsic anharmonicity and analyze the validity of the Mie-Grüneisen approximation at high temperatures.

DOI: 10.1103/PhysRevB.67.224110 PACS number(s): 64.30.+t, 62.20.Dc, 63.20.Ry, 61.50.Ks

I. INTRODUCTION

Periclase (MgO) is one of the major Earth-forming minerals. Only one solid phase, with the NaCl-type structure, has been observed, although experiments have probed temperatures up to the melting point and pressures to 227 GPa.[1] This unique structural stability suggests that MgO may remain in the NaCl structure throughout the P-T regime of the Earth's crust and mantle; it also makes MgO an ideal standard for calibrating pressure in experiments at extreme conditions. The stability and equation of state of MgO have been extensively studied theoretically[2–21] and experimentally (Refs. 1 and 22–28 to list only a few). Here we re-address these issues with advanced computational tools, such as *ab initio* molecular dynamics (AIMD) and projector augmented-wave (PAW) method. This allows us, on the one hand, to go beyond the static calculations and study thermal properties and, on the other hand, to assess the pseudopotential errors by comparing the results of pseudopotential calculations with all-electron PAW results. Our calculations are based on the generalized gradient approximation (GGA), whereas most of the previous work was done within the local density approximation (LDA). Our calculations confirm the extraordinary stability of MgO in the NaCl-type structure. AIMD simulations allowed us for the first time to evaluate the intrinsic anharmonic effects, particularly important for thermal expansion.

The electronic structure of and chemical bonding in MgO are prototypical of ionic oxides. The high ionicity of MgO follows from the large difference in the electronegativities of Mg and O,[29] and is confirmed by the analysis of the experimental equation of state,[30] calculated charge density,[31] band structures,[5] lattice dynamics,[12,32] electrostatic potentials,[9] and the wave functions.[33,34] A crucial fact is that the O^{2-} ion is unstable in the free state, but can be stabilized by the crystal electrostatic field. The properties (ionic ''size,'' strength of interaction with other ions) of the O^{2-} ion in crystals are strongly dependent on the electrostatic potential and, therefore, on the positions of all the ions. Pairwise interionic interactions change in a non-trivial way when ions are displaced or when the crystal is strained or compressed. These effects give rise to many-body forces and explain why the elastic constants of MgO and other simple alkali earth oxides have very large violations from the Cauchy relation ($C_{12} = C_{44} + 2P$). To model the elasticity of MgO realistically, one needs to go beyond the simple pair potential model with rigid ions (which is more successful in ionic fluorides than in oxides) and use such models as the breathing-shell,[11] compressible-ion,[35] or potential-induced-breathing[5,36] models, or resort to full quantum-mechanical treatments.[2,12–14,37] Using *ab initio* calculations, Karki and co-workers[2,19] reproduced the experimental elastic constants at ambient conditions and predicted that the elastic anisotropy of MgO changes sign with pressure and becomes very large by $\sim$100 GPa, making MgO the most elastically anisotropic mineral in the lowermost mantle, a conclusion questioned by Sinogeikin and Bass,[38] but supported here using more accurate calculations. This issue is important for interpreting the observed seismic anisotropy of the lowermost mantle.[39]

The aim of this paper is threefold: first, to analyze the accuracy of the computational methods used; second, to predict the properties of MgO at extreme P-T conditions where reliable experimental data are scarce—our theoretical results could then be used to constrain the temperature distribution and composition of the Earth's lower mantle; third, to assess some of the often made assumptions related to thermoelastic properties of crystals. To our knowledge, here we are reporting on the first *ab initio* calculations of the intrinsic anhar-

monicity parameter, which allowed us to perform a detailed assessment of the quasiharmonic approximation.

II. COMPUTATIONAL METHODOLOGY

The calculations performed here were based on density functional theory (DFT) (Ref. 40) within the generalized gradient approximation (GGA),[41] which is the most advanced currently available approximation in DFT. The upcoming meta-GGAs (Ref. 42) are promising, but have not yet been widely and self-consistently implemented in the existing computer packages. The GGA is known to overestimate bond lengths by ~1%, but at the same time (especially at the experimental structure) gives accurate electron densities and other quantities, including vibrational, elastic and anharmonic properties.

The calculations were performed with the VASP code.[43] Valence electron orbitals were expanded in plane waves with the kinetic energy cut-off of 500 eV (the basis set incompleteness errors are within 3 meV/atom for the total energy and 0.5 GPa for the pressure); the core orbitals were treated as ''frozen'' within the PAW formalism[44] or replaced by nonlocal effective core pseudopotentials (ECP). We use the ECPs and PAW potentials supplied with the VASP code.

In all our ECP and PAW calculations the O atom was described with a $1s^2$ core. For Mg we used two descriptions: (1) with a $1s^2 2s^2$ core (''Be core'', or ''small core'') and (2) $1s^2 2s^2 2p^6$ core (''Ne core,'' or ''large core''). Ultrasoft ECPs (Ref. 45) were used for O atoms in all ECP calculations and for Mg in small-core ECP calculations; the large-core ECP used for Mg included partial core corrections[46] and was norm-conserving.[47] In all cases similar core radii (0.8 Å for O and 1.06 Å for Mg) were used, the main difference being in the description of the core and its interaction with the valence electrons.

For the Brillouin-zone sampling we used 4×4×4 (for the NaCl-type structure) and 6×6×6 (for the CsCl-type structure) Monkhorst-Pack[48] meshes, which provide convergence of the total energy to within 0.5 meV/atom and of the pressure to 0.3 GPa. The Kohn-Sham equations were solved iteratively to self-consistency within 10^{-8} eV per unit cell. At each pressure, the elastic constants were determined from non-linear stress-strain relations.[14]

Using the *ab initio* forces on atoms, we performed *ab initio* molecular dynamics simulations in the *NVT* ensemble[49] for 2×2×2 cubic supercells (64 atoms). In these simulations, the ground state was found self-consistently (to within 10^{-8} eV/atom) at each timestep. These simulations were performed at 500, 1500, and 3000 K and volumes corresponding to the supercell parameters 7.4, 7.6, 7.8, 8.0, 8.2, 8.422, and 8.6 Å. The thermostat mass parameter was tuned so as to produce temperature oscillations with the period similar to the average period of atomic vibrations in the crystal. The time step of 1.5 fs proved to give accurate results. After equilibration (typically several hundred fs), simulations were run for another 1.5 ps. The Brillouin zone was sampled only at the Γ point, and the related error (estimated using 4×4×4 sampling and the same supercells) is less than 0.15 GPa for the pressure and 12 meV/atom for the total energy. Errors due to the finite system size and finite simulation time (estimated using molecular dynamics simulations based on a rigid-ion Buckingham potential model) are always less than 10% for the thermal pressure. We also performed static simulations for the same 2×2×2 supercells and with the same computational conditions; at each temperature the thermal pressure was obtained as the difference of pressures in the static and thermal systems:

$$P_{\mathrm{vib}}(V,T) = P(V,T) - P_{\mathrm{st}}(V). \tag{1}$$

In the first approximation (neglecting intrinsic anharmonicity), the vibrational energy of a classical system is $(3N\text{-}3)k_B T$, where N is the number of atoms in the supercell. This gives the effective Grüneisen parameter:

$$\gamma_{\mathrm{eff}}(V,T) = \frac{P_{\mathrm{vib}}(V,T)}{(3N-3)k_B T} V. \tag{2}$$

For a quasiharmonic classical solid the Grüneisen parameter depends only on volume, but due to intrinsic anharmonicity the actual $\gamma_{\mathrm{eff}}(V,T)$ has a small temperature dependence. As we show below, it is possible to extract the temperature-dependent anharmonic corrections and the temperature-independent (quasiharmonic) Grüneisen parameter from $\gamma_{\mathrm{eff}}(V,T)$.

III. STATIC EQUATION OF STATE (EOS)

Recently, it has become common to consider the Vinet EOS (Refs. 50 and 51) as the overall best EOS formulation available,[52,53] because it is based on a realistic interatomic potential function and applicable to solids with any type of chemical bonding.[54] The potential function of this EOS captures well the short-range interatomic repulsion (dominant at high pressures) and short-range attraction (as in covalent and metallic solids) but, as originally noted by Vinet *et al.*,[51] does not explicitly incorporate Coulombic (r^{-1}) and van der Waals (r^{-6}) interactions.[55] Hence, the Vinet EOS may be less successful for ionic and molecular solids at moderate pressures. To improve the situation, authors of a follow-up work[30] derived the EOS for ionic materials by augmenting the ''scaled universal energy function'' by a Coulombic term. Treating ionic charges as variables in fitting the experimental EOS data, for MgO these authors obtained charges of about +1.9 and −1.9 on Mg and O, respectively.

We find that the third-order Birch-Murnaghan EOS describes our results much better than the Vinet, logarithmic, second-order Birch-Murnaghan, or Murnaghan EOSs. For this reason, in spite of the generally higher accuracy of the Vinet EOS (which we used in our previous works[56,57]), here we preferred the third-order Birch-Murnaghan EOS (see Ref. 58):

$$P(x) = \frac{3}{2} K_0 [x^{7/3} - x^{5/3}] \{1 + \xi [x^{2/3} - 1]\}, \tag{3}$$

TABLE I. Static equation of state of MgO from different GGA calculations.

Method	V_0, Å^3	K_0, GPa	K_0'
ECP, Large-core Mg	77.629	151.707	4.212
ECP, Small-core Mg	76.595	150.839	4.052
PAW, Large-core Mg	76.049	154.183	4.141
PAW, Small-core Mg	76.947	150.597	4.103
Experiment[a]	74.712	159.94	4.112

[a]Experimental parameters at 298 K obtained by treating a large experimental P-V-T dataset (Refs. 1 and 22–26).

$$E(x)=E_0+\frac{3}{2}K_0V_0\left[\frac{3}{2}(\xi-1)x^{2/3}+\frac{3}{4}(1-2\xi)x^{4/3}+\frac{1}{2}\xi x^{6/3}-\frac{2\xi-3}{4}\right], \quad (4)$$

where $x=V_0/V$ and $\xi=\frac{3}{4}(K_0'-4)$. EOSFIT program[59] was used for fitting EOSs, the parameters of which are listed in Table I. It is interesting to note that LDA pseudopotential results of our recent study[21] are, on the contrary, better described by the Vinet EOS.

Figure 1 shows EOSs obtained in different series of calculations. Small-core PAW calculations should be comparable in accuracy to the best all-electron calculations. The excellent performance of large-core PAW calculations suggests that core deformation effects are not significant. Large-core ECP results are visibly different from results of all the other, more accurate, calculations. The atomic core regions begin to overlap only at pressures above 150 GPa, but the errors of large-core pseudopotentials are significant already at much lower pressures.

It emerges that a major source of errors of the large-core ECP calculations for MgO is related to the overlap of the semicore 2p orbitals of Mg and its valence orbitals, the associated problems being only partly remedied by nonlinear core corrections.[46] These errors change the ''effective size'' of the Mg atom in large-core ECP calculations. Overlap between the Mg 2p orbitals and the valence orbitals of the neighboring O atoms, rapidly increasing on compression and not properly treated in large-core ECP calculations, may explain the observed increase of the pseudopotential errors with pressure (Fig. 1). These effects should be less significant in situations where Mg atoms are situated in large cavities with long Mg-O bonds (as in $Mg_3Al_2[SiO_4]_3$ pyrope or $MgSiO_3$ perovskite). Indeed, we found the pseudopotential errors for $MgSiO_3$ perovskite to be within 3 GPa for the EOS calculated up to ~150 GPa. In what follows, we discuss and compare only the results of small-core PAW and large-core ECP calculations.

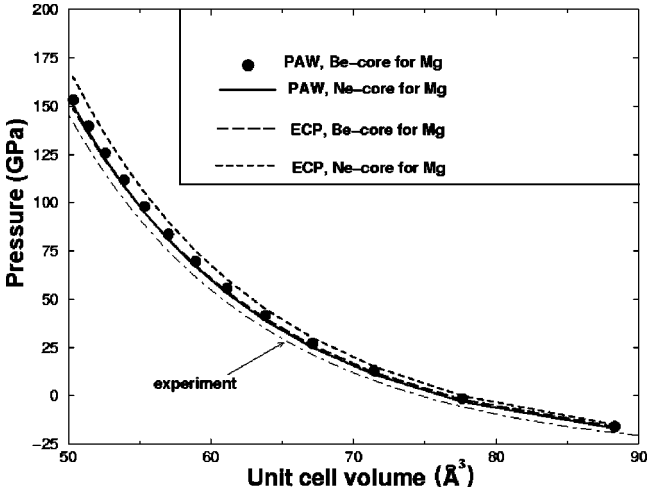

FIG. 1. Equation of state of MgO: theory and experiment.

IV. B1-B2 TRANSITION PRESSURE

There are many examples of ionic crystals with the NaCl (''B1'') structure, which at high pressure transform into the CsCl (''B2'') structure. From theoretical calculations, in MgO this transition is expected at very high pressures, not yet probed by experiments. However, the estimates from different calculations (Table II) range from 200 to over 1000 GPa. This is partly due to the diversity of methods used and partly due to small basis sets and other limitations on the accuracy of the early calculations;[6,16,17] the pseudopotential error can also be large. The most accurate all-electron calculations give transition pressures of ~510 GPa.[4,5] Our small-core PAW calculations (see Fig. 2) give $P_{tr}=509$ GPa, our large-core ECP result is 20 GPa lower, $P_{tr}=489$ GPa. Volume and energy differences between the B1 and B2 phases at the transition pressure are very similar in our PAW and large-core ECP calculations: $(\Delta V/V)(P_{tr})=4.6\%$ (ECP) and 4.8% (PAW), $\Delta E(P_{tr})=1.32$ eV per formula unit in both ECP and PAW calculations.

Our recent LDA pseudopotential calculations[21] have also resulted in a similar static transition pressure of 490 GPa. As shown by our *ab initio* lattice dynamics calculations,[21] the inclusion of zero-point energy lowers this by 16 GPa. Thermal effects further lower the transition pressure (see Ref. 21 for a theoretical phase diagram); however, at all conditions relevant to the Earth the B1 phase remains thermodynamically stable.

V. ELASTIC CONSTANTS

MgO is cubic and its second-rank tensor properties (e.g., thermal expansion, dielectric constants, and compressibility) are isotropic. However, elasticity, being a fourth-rank tensor property, is anisotropic even for cubic crystals, where it is conveniently expressed[2] by the dimensionless parameter $A=[(2C_{44}-C_{12})/C_{11}]-1$. MgO turns out to be elastically highly anisotropic at ambient conditions.

Karki *et al.*[2] predicted a qualitative change of anisotropy with pressure: at moderate pressures, A decreases to zero at ~20 GPa, changes sign, and by ~100 GPa (which corresponds to the bottom of the Earth's mantle) adopts large negative values, making MgO probably the most elastically anisotropic mineral in the Earth's lowermost mantle. Thermal effects do not change this conclusion.[13,60] Following this prediction, the elastic constants of MgO were measured up to

TABLE II. Theoretical B1-B2 transition pressure.

Method	P_{tr} GPa
GGA calculations	
GGA-PAW	509[a]
GGA-ECP plane wave	489[a]
GGA-ECP plane wave	664[b]
GGA-ECP plane wave	400[c]
GGA-LCAO	515[d]
GGA-LCAO	428 (PBE), 418 (PW91)[e]
LDA calculations	
LDA-LAPW	510[f]
LDA-LCAO	515[d]
LDA-LCAO	512[e]
LDA-ECP plane wave	490 (474)[g]
LDA-ECP plane wave	451[h]
LDA-LMTO	198[i]
LDA-ECP plane wave	1050[j]
Hartree-Fock (HF) calculations	
HF-LCAO	712[d]
HF-LCAO	220[k]
Other methods	
Modified PIB	580[l]
Modified LDA	370[m]

[a]This work.
[b]Reference 15.
[c]Reference 18.
[d]Reference 4.
[e]Reference 3.
[f]Reference 5.
[g]Reference 21. In parentheses—including zero-point energy.
[h]Reference 2.
[i]Reference 16.
[j]Reference 6.
[k]Reference 17.
[l]Reference 9.
[m]Reference 7.

18.6 GPa (Ref. 38) and up to 55 GPa (Ref. 27) using Brillouin spectroscopy. Experiments agreed with theory below ~20 GPa, but at higher pressures showed large differences and suggested that MgO is much less elastically anisotropic than predicted in Ref. 2.

We calculate the elastic constants of MgO similarly to Ref. 2, but using the GGA (rather than the LDA) and both all-electron (PAW) and ECP calculations (only ECP calculations were used in Ref. 2). This allows us to evaluate the pseudopotential errors in the calculated elastic constants and to check calculations of Ref. 2. Our results are shown in Table III and Fig. 3; the latter shows that all theoretical calculations (LDA and GGA, ECP and PAW) agree very well with each other and with experiments[27,38] below 20 GPa.

Like Karki *et al.*,[2] we find large Cauchy violations increasing in absolute value with pressure. Our all-electron GGA calculations almost exactly reproduce the experimental[27,38] anisotropy factor below ~20 GPa.

Above 20 GPa, results of Zha *et al.*[27] depart significantly from all theoretical predictions and give non-monotonic dependences of the Cauchy deviations and anisotropy factors on pressure. While the accuracy of *ab initio* calculations should not depend on pressure, experiments are problematic at high pressures (in particular, due to nonhydrostaticity) and, as documented in Ref. 27, have large error bars (a ~15–20% error for C_{12}).

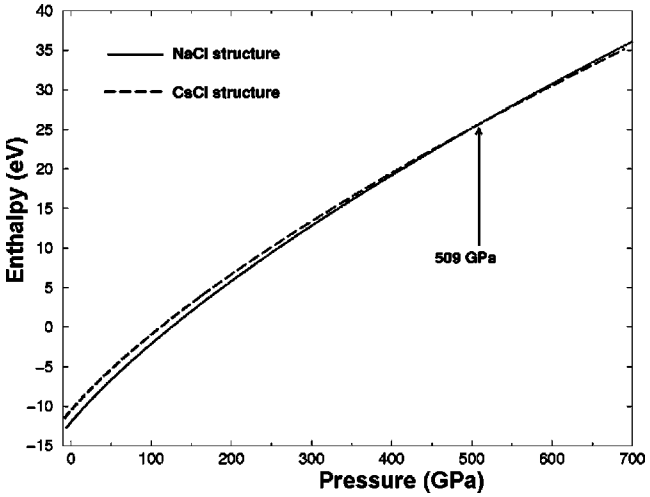

FIG. 2. $H(P)$ curves of MgO polymorphs (small-core PAW calculations).

Simultaneously measuring the elastic constants (from which the bulk modulus K was calculated) and lattice parameters, Zha *et al.*[27] derived the EOS of MgO without using any pressure standards. This EOS relied on the accuracy of their measured bulk modulus and was used to recalibrate the ruby pressure scale. We find that unlike the individual elastic constants, the bulk modulus of Ref. 27 agrees with theory. It seems that the errors in their experimental elastic constants are somehow averaged out when the bulk modulus is calculated. Therefore our calculations support the primary pressure scale suggested by Zha *et al.*,[27] even though the individual elastic constants of Ref. 27 do not agree with our calculations at high pressures.

VI. THERMAL EQUATION OF STATE AND ANHARMONIC EFFECTS

The total free energy can be expressed as a sum of the static (F_{st}), quasiharmonic (F_{qh}), and anharmonic (F_a) terms

$$F_{vib}(V,T)=F_{st}(V)+F_{qh}(V,T)+F_a(V,T), \tag{5a}$$

and the total pressure is then a sum of a static, quasiharmonic, and anharmonic terms:

$$P(V,T)=-\left(\frac{\partial F}{\partial V}\right)_T=P_{st}(V)+P_{qh}(V,T)+P_a(V,T). \tag{5b}$$

For the quasiharmonic part, the Mie-Grüneisen equation is valid (rigorously in the high-temperature limit):

TABLE III. Elastic constants of MgO predicted at the GGA level of theory. PAW results. At $a_0 = 4.211$ Å (experimental lattice parameter at ambient conditions) are also given: large-core ECP results (in parentheses) and experimental results (Ref. 38) (in brackets). The elastic constants are in GPa.

a_0, Å	V_0, Å^3	P, GPa	C_{11}	C_{12}	C_{44}	K	G	$C_{12}-C_{44}-2P$	A	θ_D, K
4.3	79.51	−4.82	235.8	82.0	136.7	133.3	108.5	−45	0.51	866
4.2513	76.84	0	279.9	90.9	142.5	153.9	120.9	−52	0.34	910
4.211	74.67	4.72	320.2	98.5	147.6	172.4	131.6	−59	0.23	945
		(6.40)	(338.9)	(98.6)	(145.5)	(178.7)	(134.8)	(−60)	(0.15)	(957)
		[0; 300 K]	[297.8]	[95.8]	[154.7]	[163.1]	[130.4]	[−58.9]	[0.36]	[940]
4.10	68.92	20.73	449.3	120.9	158.5	230.4	160.8	−79	−0.03	1033
4.0	64.00	40.58	620.3	150.9	171.7	307.3	194.6	−102	−0.20	1126
3.9	59.32	66.94	816.8	183.6	183.3	394.7	228.5	−134	−0.33	1207
3.8	54.87	102.49	1098.4	227.5	197.8	517.8	272.9	−175	−0.43	1305
3.7	50.65	149.26	1423.7	283.3	208.2	663.4	316.0	−223	−0.52	1389

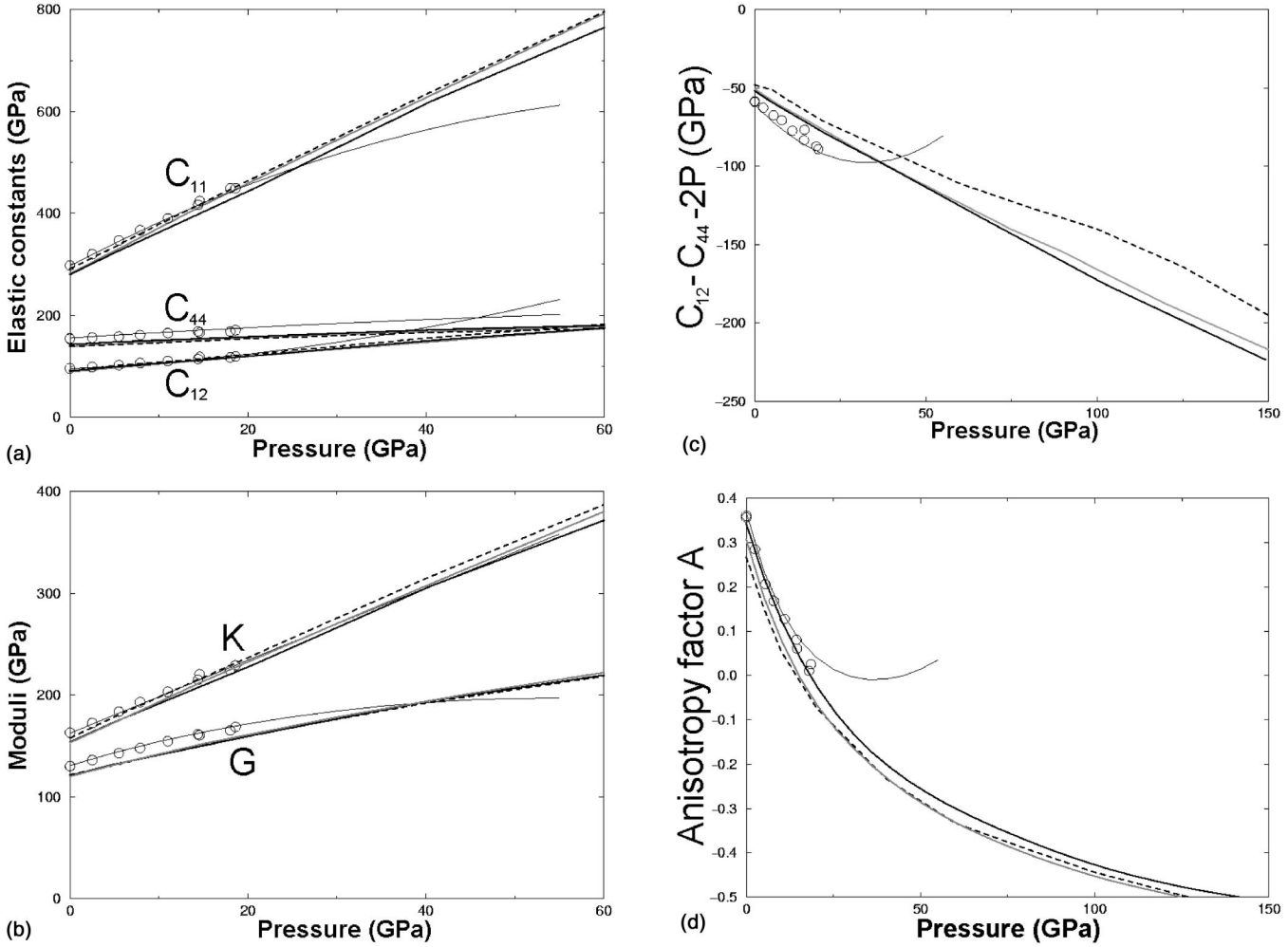

FIG. 3. Elasticity of MgO. (a) Elastic constants. (b) Bulk and shear moduli. (c) Cauchy violations. (d) Anisotropy parameter A. Theory: *solid lines*—this work (*black*—PAW, *gray*—ECP calculations); *dashed lines*—LDA results (Ref. 2). Experiment: *thin lines* (Ref. 27), *circles* (Ref. 38).

$$P_{\mathrm{qh}}(V,T)=\frac{E_{\mathrm{vib}}^{\mathrm{qh}}}{V}\gamma_{\mathrm{qh}}(V), \tag{6}$$

where $E_{\mathrm{vib}}^{\mathrm{qh}}$ is the (quasiharmonic) vibrational energy and $\gamma_{\mathrm{qh}}(V)$ the (quasiharmonic) Grüneisen parameter.

For the anharmonic part, which is important only at high temperature, we use the classical approximation and the lowest-order perturbation theory, in which the anharmonic free energy and pressure are quadratic in temperature:[61–63]

$$F_a(V,T)=\frac{3}{2}Nk_BaT^2 \tag{7}$$

and

$$P_a(V,T)=-\frac{3}{2}Nk_B\frac{d\ln a}{d\ln V}a(V)\frac{T^2}{V}, \tag{8}$$

where a is the intrinsic anharmonicity parameter. This parameter can be related to the temperature change of the phonon spectrum[63] and plays a central role in the present treatment of anharmonicity.

The total pressure is then

$$P(V,T)=P_{\mathrm{st}}(V)+\frac{E_{\mathrm{vib}}^{\mathrm{qh}}}{V}\gamma_{\mathrm{qh}}(V)-\frac{3}{2}Nk_B\frac{d\ln a}{d\ln V}a(V)\frac{T^2}{V}. \tag{9}$$

The quasiharmonic vibrational energy $E_{\mathrm{vib}}^{\mathrm{qh}}$ can be calculated from the phonon spectrum or from some simplified models—e.g., the Debye model. At high temperatures $E_{\mathrm{vib}}^{\mathrm{qh}}=3Nk_BT$. High temperatures present a very special case—first, because many applications of our work are intended for high temperatures of the Earth's interior, second, because at high temperatures the quantum vibrational effects vanish and the resulting classical theory and its equations become very easy to work with and, third, because molecular dynamics method employed here is based on the classical approximation. Combining the classical equations with AIMD results, we determine the parameters $\gamma(V)$ and $a(V)$, which are then used to construct the EOS.

In the classical approximation, $E_{\mathrm{vib}}^{\mathrm{qh}}=3Nk_BT$, and Eq. (9) may be rewritten for the vibrational pressure as follows:

$$P_{\mathrm{vib}}(V,T)=\frac{3Nk_BT}{V}\left[\gamma_{\mathrm{qh}}(V)-\frac{1}{2}a\frac{d\ln a}{d\ln V}T\right]. \tag{10}$$

In Eq. (10), the factor $3N$ denotes the number of vibrational degrees of freedom (per N atoms). A subtlety is that in molecular dynamics (MD) simulations, due to the finite supercell size and the constraint that the total crystal momentum be always zero, the number of degrees of freedom is decreased to $3N-3$. Therefore, instead of $3N$, the factor of $(3N-3)$ should be used in Eq. (10) whenever it is applied to MD results;[64] such a modification can be seen in Eq. (2). The expression in brackets in Eq. (10) is the effective Grüneisen parameter defined in Eq. (2), and now it is clear that its dependence is solely due to intrinsic anharmonicity:

$$\gamma_{\mathrm{eff}}(V,T)=\gamma_{\mathrm{qh}}(V)-\frac{1}{2}a\frac{d\ln a}{d\ln V}T. \tag{11}$$

The effective Grüneisen parameters were calculated at a series of volumes as described in Sec. II. The results (Fig. 4) show some temperature dependence due to intrinsic anharmonicity.

From γ_{eff} calculated at different volumes and temperatures, using Eq. (11) we find $\gamma_{\mathrm{qh}}(V)$ and $a(V)$. The intrinsic anharmonic parameter was fitted to $a=a_0(V/V_0)^m$; due to its smallness, it could be determined only with errors as large as 30–50%.

A rigorous functional form of the Grüneisen parameter, although very desirable for many purposes, is not known. A simple function, that describes theoretical data (including ours) very well and that is well-behaved at infinite compressions, was suggested by Al'tshuler *et al.*[65] and Vorobev:[66]

$$\gamma=\gamma_\infty+(\gamma_0-\gamma_\infty)\left(\frac{V}{V_0}\right)^\beta, \tag{12}$$

where γ_0 and γ_∞ are values of the Grüneisen parameter at $V/V_0=1$ (ambient conditions) and 0 (infinite compression) respectively, $V_0=74.672$ Å^3, and β is a fitted parameter. Resulting values of the parameters are given in Table IV. The agreement with experiment is good for γ_0 and semiquantitative for a_0 and m. The values of γ_∞ and β seem to agree between experiment and ECP calculations, but differ from the more accurate PAW calculations.[67] This may be due to the difficulties in obtaining these parameters from experiment.[68] The experimental value of γ_0, on the other hand, is known very well: its experimental estimate[70] is $\gamma_0=1.54(\pm0.08)$, and the previous theoretical estimate[15] is $\gamma_0=1.542$.

PAW and large-core ECP calculations give practically identical results for the Grüneisen parameter at low pressures, but the differences increase on compression and at $V/V_0<0.85$ become significant (Fig. 4). This again may be ascribed to the overlap of the oxygen 2p-orbitals with the semicore 2p orbitals of Mg, which is neglected in large-core ECP calculations.

From our results we see, first of all, that at low pressures the effective Grüneisen parameter significantly depends on temperature, but this dependence (which is due to intrinsic anharmonicity) is suppressed at high pressure (Fig. 4). Figure 5 shows that quasiharmonic thermal pressure is a very important contribution, while intrinsic anharmonic pressure is small even at very high temperatures (within 2.7 GPa at 3000 K).

Our model thermal EOS includes the following ingredients: (1) GGA-PAW static pressure, (2) GGA-PAW Grüneisen parameter and intrinsic anharmonic parameter (as function of volume) and (3) quasiharmonic thermal energy calculated with the Debye model (the Debye temperature θ_D is calculated from *ab initio* elastic constants at each volume—Table III). The Debye model introduces quantum phonon corrections in a simple way; for the vibrational en-

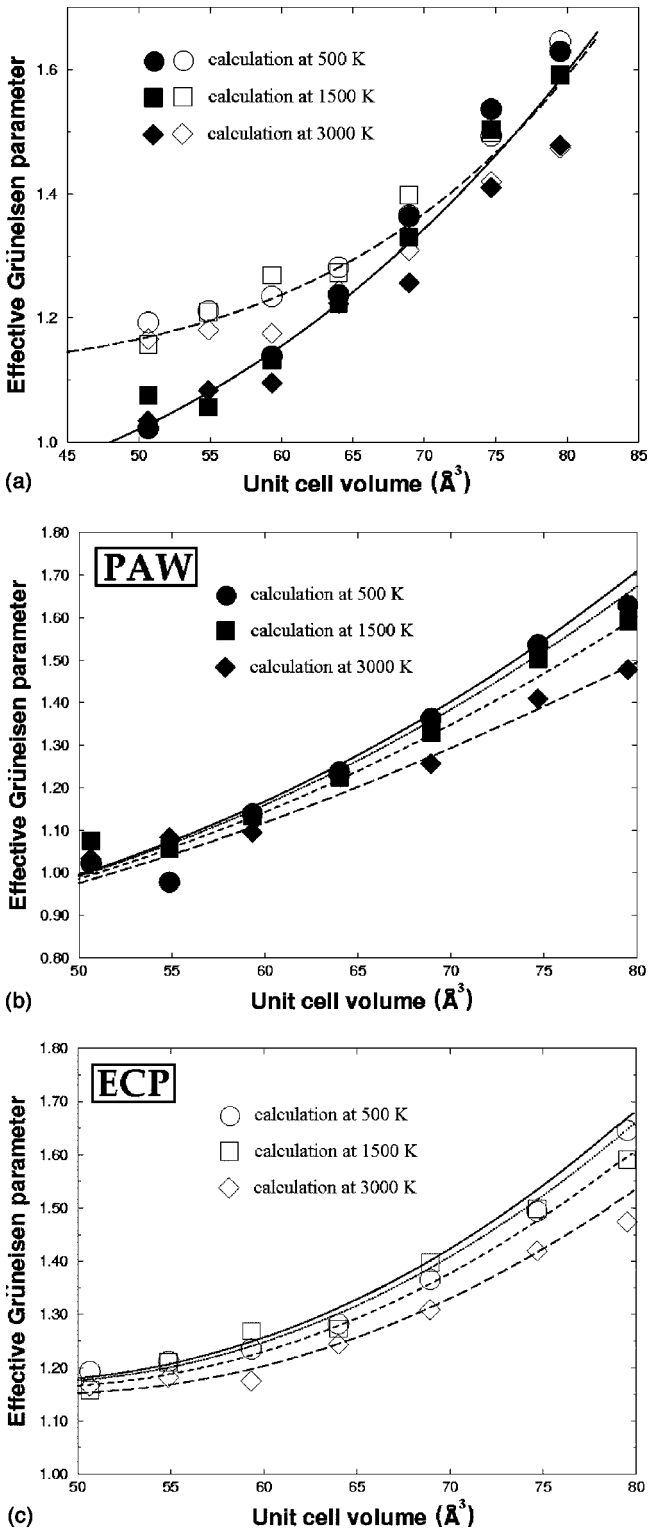

FIG. 4. Effective Grüneisen parameter of MgO. (a) Best fit lines for the *effective* Grüneisen parameter are well described by function (13) with $\gamma_0=1.455$ (1.459), $\gamma_\infty=0.841$ (1.113), and $\beta=3.057$ (4.673) for PAW (ECP) calculations. *Filled symbols*—PAW, *open*—ECP calculations. (b) PAW and (c) ECP results. *Lines*—model (12).

TABLE IV. Volume dependence of the quasiharmonic Grüneisen parameter and intrinsic anharmonic parameter.

Method	γ_0	γ_∞	β	a_0, 10^{-5} K^{-1}	m
ECP	1.527	1.152	5.594	1.771	4.989
PAW	1.537	0.745	2.869	1.969	5.127
Expt.[a]	1.563	1.248	6.064	1.427	6.090

[a]Dorogokupets & Oganov (in prep.).

ergy it gives the correct low-temperature T^4 law, the exact high-temperature limit, and reasonable behavior at intermediate temperatures.

The GGA is known to systematically overestimate lattice parameters by 1–2%, and this is also the case for MgO. As in our previous study of $MgSiO_3$ perovskite,[57] we find that a constant shift of the static pressure (for PAW calculations by

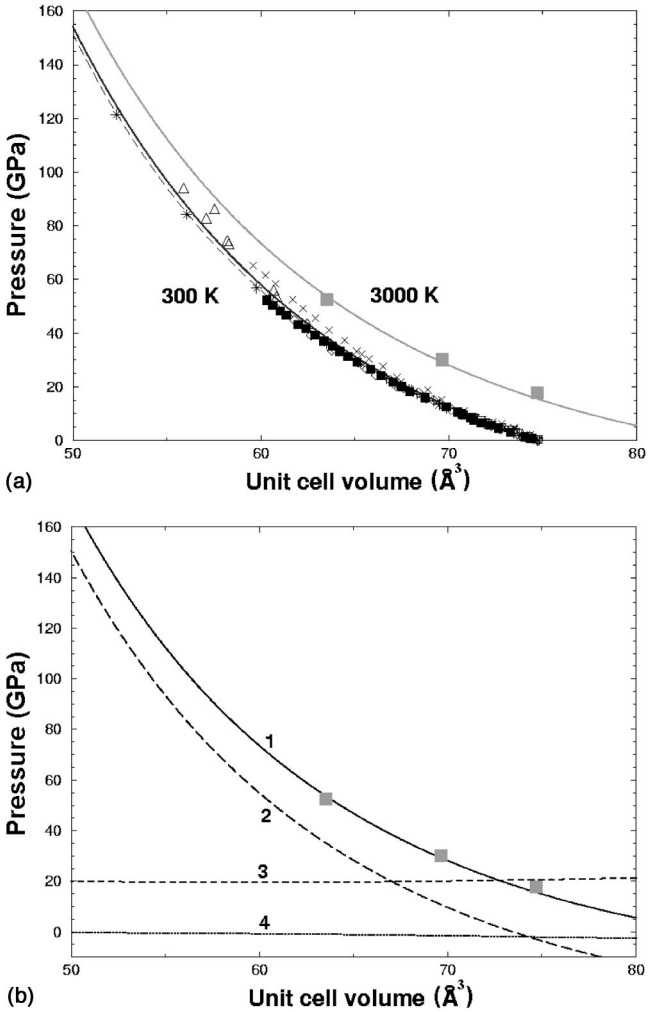

FIG. 5. Equation of state of MgO. (a) Total pressure at 300 and 3000 K. *Solid lines*—pressure-corrected theory (this work: black line—300 K, gray—3000 K), dashed—experiment at 300 K. *Black symbols*—experimental data (Refs. 1 and 22–26) at 300 K, *large gray squares*—extrapolation (Ref. 22) at 3000 K. (b) Total pressure at 3000 K (line 1); static pressure (2), quasiharmonic (3) and anharmonic (4) thermal pressure contributions.

TABLE V. Pressure-corrected EOS in the BM3 parametrization at several temperatures.

T, K	V_0, Å^3	K_0, GPa	K_0'
Static	73.425	181.240	3.997
0	74.439	173.480	4.014
298	74.670	170.530	4.036
1000	76.549	152.595	4.130
2000	79.915	127.719	4.244
3000	83.772	106.110	4.331
4000	88.006	88.473	4.385

−7.736 GPa to match the experimental unit cell volume at ambient conditions) corrects for the main part of this error. With this pressure correction, we calculated the EOS of MgO. Table V gives parameters of the third-order Birch-Murnaghan fits to the thermal EOS. Figure 5 shows that the agreement between our calculated EOS at 300 and 3000 K and experimental results is very satisfactory. Comparing our model EOS with direct AIMD results at 4500 K and three different volumes, we found agreement within 2–3 GPa.

Figure 6 shows the calculated (this work and Refs. 12 and 13) and experimental[28] thermal expansion. One can see that the neglect of intrinsic anharmonicity in the quasiharmonic approximation leads to an overestimation of thermal expansion,[12,13] rather spectacular at low pressures, but small at high pressures, where all anharmonic effects are suppressed. Our calculations show that including intrinsic anharmonicity we closely reproduce experimental values; setting the intrinsic anharmonicity to zero, we recover the quasiharmonic results.[12,13]

As shown by Holzapfel,[54] the three common definitions of the Grüneisen parameter (via the thermal pressure, thermal expansion, and volume derivatives of the phonon frequencies)

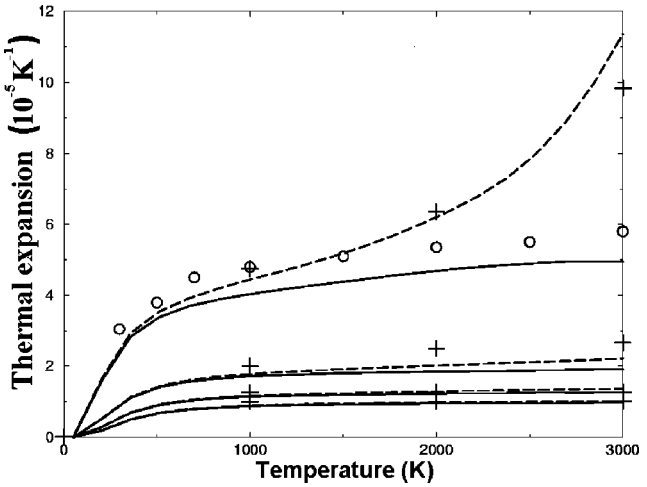

FIG. 6. Thermal expansion of MgO. Results are presented for 0, 50, 100, and 150 GPa (from top to bottom): *solid lines*—calculations with intrinsic anharmonicity (this work), *dashed lines*—quasiharmonic model (this work), *crosses*—quasiharmonic calculations (Refs. 12 and 13). Experimental data at 1 atm (Ref. 28) are shown by circles.

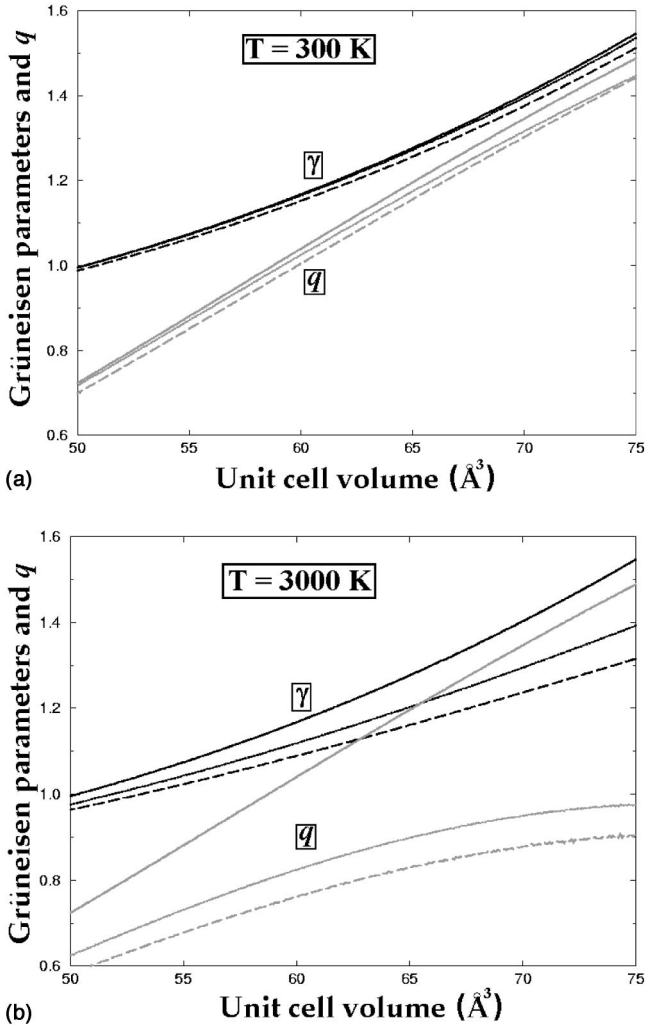

FIG. 7. Grüneisen parameters and $q=(\partial \ln \gamma/\partial \ln V)_T$ of MgO as a function of volume. (a) At 300 K. (b) At 3000 K. *Solid lines*—quasiharmonic results [cf. Eq. (13c)], *dotted lines*—calculated using Eq. (13b), *dashed lines*—calculated using Eq. (13a). Black lines—γ, gray—q.

$$\gamma_P(V,T)=\frac{P_{\rm th}}{E_{\rm th}}V, \tag{13a}$$

$$\gamma_\alpha(V,T)=\alpha\frac{K_T V}{C_V}, \tag{13b}$$

$$\gamma_{\rm qh}(V)=\left\langle -\frac{d\ \ln\ \omega_i}{d\ \ln V}\right\rangle \tag{13c}$$

are all identical in a classical quasiharmonic solid, and all different in a system with intrinsic anharmonicity. Very roughly, $\gamma_P(V,T)$ is halfway between $\gamma_{\rm qh}(V)$ and $\gamma_\alpha(V,T)$, i.e., anharmonic effects are much more pronounced in thermal expansion than in thermal pressure. We stress that care must be taken as to which definition of the Grüneisen parameter is used when analyzing experimental and theoretical results. Figure 7 shows the different definitions of the Grün-

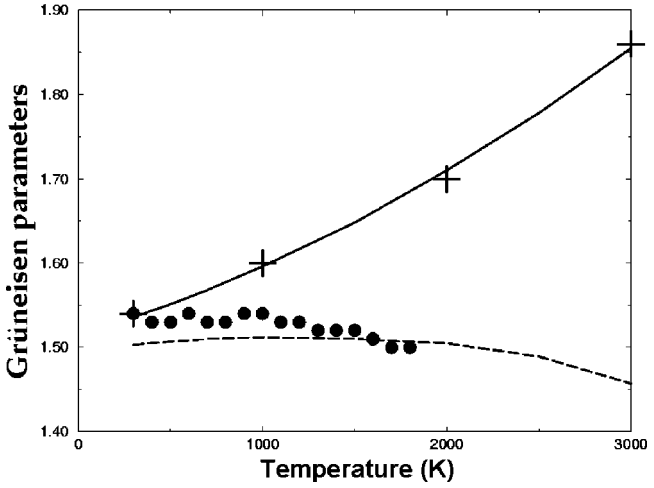

FIG. 8. Grüneisen parameter of MgO at 0 GPa. *Solid line*—quasiharmonic Grüneisen parameter γ_{qh} (this work); *crosses*—quasiharmonic calculations (Refs. 12 and 13), *dashed line*—fully anharmonic calculation of $\gamma_\alpha(V,T)$ (this work). *Solid circles*—experimental $\gamma_\alpha(V,T)$ (Ref. 70).

eisen parameter and that the differences are small at low temperatures, but significantly increase with temperature. In Fig. 7 we also show the volume dependence of the parameter q:

$$q=\left(\frac{\partial \ln \gamma}{\partial \ln V}\right)_T. \tag{14}$$

Figure 7 shows that the often used assumption that q = const (often taken to be 1—see, e.g., Ref. 69) is very crude; it is not possible to fit theoretical data well with such an assumption. It is also obvious that q strongly depends on which definition of the Grüneisen parameter is used in Eq. (14). In the quasiharmonic approximation, q is temperature independent; intrinsic anharmonicity results in a strong temperature dependence of q derived from $\gamma_P(V,T)$ or $\gamma_\alpha(V,T)$, whereas q derived from $\gamma_{\rm qh}(V)$ has no explicit temperature dependence.

Experimental and theoretical values of the Grüneisen parameter of MgO are compared in Fig. 8. Karki *et al.*[12] found that the quasiharmonic approximation cannot reproduce the experimental data.[70] Indeed, setting the intrinsic anharmonic effects in our model EOS to zero, we arrived at the values of the Grüneisen parameter practically identical to those obtained by Karki *et al.*[12] and very different from experimental data[70] at high temperatures. Including the intrinsic anharmonic effects and considering $\gamma_\alpha(V,T)$ (which is what was determined in Ref. 70), we get a perfect (well within the experimental error of ± 0.08) agreement with experiment, showing that our intrinsic anharmonic parameters must be quite accurate. We would like to stress again the differences in the conventional definitions of the Grüneisen parameter and the fact that thermal expansion is more sensitive to intrinsic anharmonic effects than thermal pressure.

It is instructive to look at the heat capacities C_V and C_P (Fig. 9). C_V at high temperatures (or, rather, its deviations

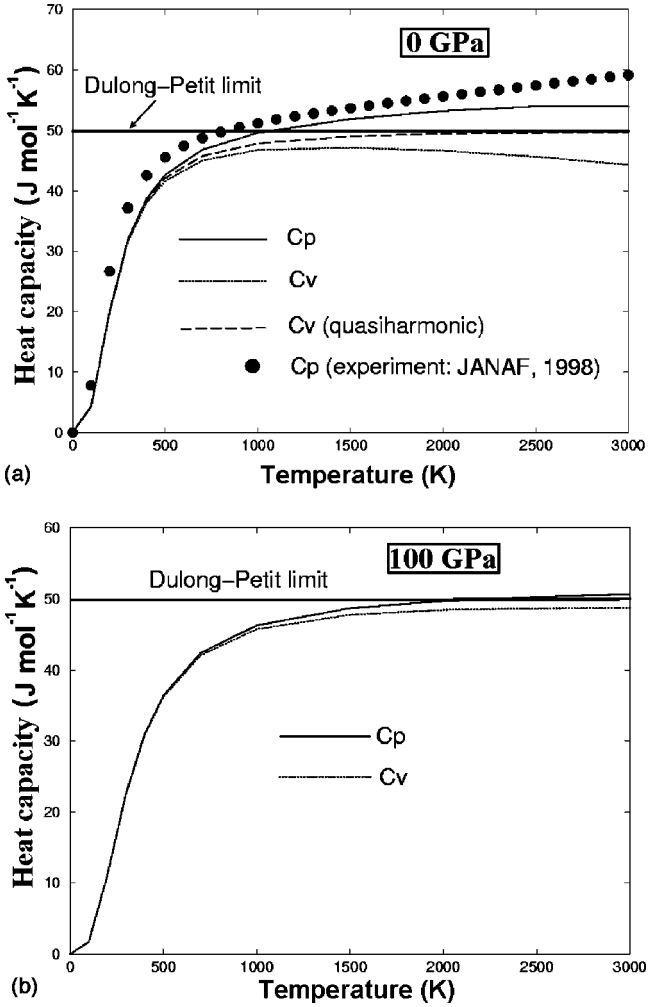

FIG. 9. Heat capacities C_V and C_P (a) at 0 GPa and (b) at 100 GPa. Experimental values of C_P are from the NIST-JANAF tables (Ref. 71).

from the Dulong-Petit limit) gives direct information on the intrinsic anharmonic effects. However, it is C_P that is experimentally measured, and C_P contains both intrinsic anharmonic and quasiharmonic contributions leading to the departure from the Dulong-Petit law; often it is difficult to separate these contributions accurately. First of all, from Fig. 9 one can see that experimental and theoretical values of C_P are rather close. At low temperatures the differences are due to the approximations of the Debye model used here; at high temperatures most of the difference can be reduced to the experimental errors and theoretical errors in the Grüneisen parameter and intrinsic anharmonicity parameter. One can also see that intrinsic anharmonicity lowers the heat capacity [compare quasiharmonic C_V and C_V calculated including intrinsic anharmonicity in Fig. 9(a)]. Figure 9(b) illustrates that all the anharmonic effects are suppressed at high pressures and both C_V and C_P are very close to the Dulong-Petit limit at high pressures and temperatures.

VII. CONCLUSIONS

We have calculated a number of properties of periclase (MgO) using density functional theory at the GGA level,

using pseudopotential and all-electron PAW methods. We find that it is important to treat the semicore 2p states of the Mg atom explicitly. Large-core ECP calculations have significant errors for most properties of MgO, especially at high pressures. These errors are due to the overlap between the Mg 2p orbitals and valence orbitals of the same Mg atom as well as of the neighboring O atoms. Such errors are expected to be much less significant when Mg occupies large cavities in structures (like in $MgSiO_3$ perovskite or in $Mg_2Al_2[SiO_4]_3$ pyrope), and our calculations showed a very small difference between the large-core ECP and small-core PAW calculations for $MgSiO_3$ perovskite. We expect particularly large pseudopotential errors in such crystals as $MgAl_2O_4$ spinel, where Mg occupies relatively small tetrahedral positions.

From PAW calculations, we predict a B1–B2 transition in MgO at 509 GPa, which coincides with the most accurate previous theoretical estimates (510–515 GPa). The effect of temperature on the B1–B2 phase equilibrium has been studied in works,[15,18] but their results did not agree well with each other. We deal with this issue in a separate paper.[21]

Our calculated elastic constants are in good agreement with experiment and with previous LDA calculations.[2] Agreement with the experimental elastic constants[27,38] up to ~20 GPa is good, but large differences from the results of Ref. 27 are seen at higher pressures. However, the experimental bulk moduli[27,38] are close to theoretical results, and we conclude that the primary pressure scale[27] should be accurate, unlike the individual high-pressure elastic constants of Ref. 27. We confirm conclusions of Ref. 2 about the high-pressure reversal of the sign of elastic anisotropy in MgO and the prediction that MgO has a large elastic anisotropy in the lowermost mantle.

We have presented a detailed study of the thermal EOS of state of MgO. The calculated Grüneisen parameter is in agreement with previous calculations[12] and experiment.[70] The intrinsic anharmonic effects in MgO are found to be quite small for the pressure (which justifies the Mie-Grüneisen approximation for the EOS), but very important for the thermal expansion. Intrinsic anharmonicity leads to differences between the three conventional definitions of the Grüneisen parameter (the quasiharmonic definition and the definitions via thermal expansion and thermal pressure). We find that $q=(\partial \ln \gamma/\partial \ln V)_T$ is also definition-dependent and varies strongly with volume, contrary to the common assumption that $q=\text{const}$.

Our calculated thermoelastic parameters are in good agreement with well-established experimental data; for other properties we have made reliable predictions. High-pressure thermoelastic properties of MgO determined here complement those previously determined for $MgSiO_3$ perovskite[57,72] and can now be used for modeling the composition and temperature distribution in the Earth's lower mantle.

ACKNOWLEDGMENTS

Funding from NERC (Grant No. GR3/12083) and RFBR (Grant No. 02-05-64062) is gratefully acknowledged. We thank S. J. Clark, G. J. Ackland, W. B. Holzapfel, M. J. Gillan, and G. D. Price for discussions, and Academician F. A. Letnikov for his support. NERC has provided access to supercomputers of CSAR at Manchester University Computer Center via the Computational Mineral Physics Consortium.

*Corresponding author. Present address: Laboratory of Crystallography, Department of Materials, ETH Zurich, CH-8092 Zurich, Switzerland. Email address: a.oganov@mat.ethz.ch

[1] T. S. Duffy, R. J. Hemley, and H.-K. Mao, Phys. Rev. Lett. **74**, 1371 (1995).
[2] B. B. Karki, L. Stixrude, S. J. Clark, M. C. Warren, G. J. Ackland, and J. Crain, Am. Mineral. **82**, 51 (1997).
[3] M.-P. Habas, R. Dovesi, and A. Lichanot, J. Phys.: Condens. Matter **10**, 6897 (1998).
[4] J. E. Jaffe, J. A. Snyder, Z. Lin, and A. C. Hess, Phys. Rev. B **62**, 1660 (2000).
[5] M. J. Mehl, R. E. Cohen, and H. Krakauer, J. Geophys. Res. **93**, 8009 (1988).
[6] K. J. Chang and M. L. Cohen, Phys. Rev. B **30**, 4774 (1984).
[7] P. Cortona and A. V. Monteleone, J. Phys.: Condens. Matter **8**, 8983 (1996).
[8] D. G. Isaak, R. E. Cohen, and M. J. Mehl, J. Geophys. Res. B **95**, 7055 (1990).
[9] H. Zhang and M. S. T. Bukowinski, Phys. Rev. B **44**, 2495 (1991).
[10] I. Inbar and R. E. Cohen, Geophys. Res. Lett. **22**, 1533 (1995).
[11] M. Matsui, S. C. Parker, and M. Leslie, Am. Mineral. **85**, 312 (2000).
[12] B. B. Karki, R. M. Wentzcovitch, S. de Gironcoli, and S. Baroni, Phys. Rev. B **61**, 8793 (2000).
[13] B. B. Karki, R. M. Wentzcovitch, S. de Gironcoli, and S. Baroni, Science **286**, 1705 (1999).
[14] B. B. Karki, L. Stixrude, and R. M. Wentzcovitch, Rev. Geophys. **39**, 507 (2001).
[15] N. D. Drummond and G. J. Ackland, Phys. Rev. B **65**, 184104 (2002).
[16] G. Kalpana, B. Palanivel, and M. Rajagopalan, Phys. Rev. B **52**, 4 (1995).
[17] M. Causà, R. Dovesi, C. Pisani, and C. Roetti, Phys. Rev. B **33**, 1308 (1986).
[18] A. Strachan, T. Çağin, and W. A. Goddard III, Phys. Rev. B **60**, 15 084 (1999).
[19] B. B. Karki, Ph.D. thesis, University of Edinburgh, 1997.
[20] A. R. Oganov, Ph.D. thesis, University of London, 2002.
[21] A. R. Oganov, M. J. Gillan, and G. D. Price, J. Chem. Phys. **118**, 10 174 (2003).
[22] S. Speziale, C.-S. Zha, T. S. Duffy, R. J. Hemley, and H.-K. Mao, J. Geophys. Res. B **106**, 515 (2001).
[23] A. Dewaele, G. Fiquet, D. Andrault, and D. Hausermann, J. Geophys. Res. B **105**, 2869 (2000).
[24] H.-K. Mao and P. Bell, J. Geophys. Res. **84**, 4533 (1979).
[25] W. Utsumi, D. J. Weidner, and R. C. Liebermann, in *Properties of Earth and Planetary Materials at High Pressure and Temperature* (Geophys. Monogr. Ser., v. 101), edited by M. H. Manghnani and T. Yagi (Am. Geophys. Union, Washington, D.C., 1998), pp. 327–333.

[26] Y. Fei, Am. Mineral. **84**, 272 (1999).
[27] C.-S. Zha, H.-K. Mao, and R. J. Hemley, Proc. Natl. Acad. Sci. USA **97**, 13 494 (2000).
[28] G. Fiquet, P. Richet, and G. Montagnac, Phys. Chem. Miner. **27**, 103 (1999).
[29] L. Pauling, *The Nature of the Chemical Bond* (Cornell University Press, Ithaca, NY, 1960).
[30] H. Schlosser and J. Ferrante, Phys. Rev. B **48**, 6646 (1993).
[31] L. L. Boyer, Phys. Rev. B **27**, 1271 (1983).
[32] O. Schütt, P. Pavone, W. Windl, K. Karch, and D. Strauch, Phys. Rev. B **50**, 3746 (1994).
[33] F. Illas, A. Lorda, J. Rubio, J. B. Torrance, and P. S. Bagus, J. Chem. Phys. **99**, 389 (1993).
[34] All the listed works show that MgO is ~90–100% ionic. Interestingly, authors of Ref. 18, using a ''charge equilibration'' method, obtained charges of +0.7 and −0.7 on Mg and O, respectively, i.e., only ~35% ionicity.
[35] A. J. Rowley, P. Jemmer, M. Wilson, and P. A. Madden, J. Chem. Phys. **108**, 10 209 (1998).
[36] M. S. T. Bukowinski, Annu. Rev. Earth Planet Sci. **22**, 167 (1994).
[37] A. Lichanot, Solid State Commun. **116**, 543 (2000).
[38] S. V. Sinogeikin and J. D. Bass, Phys. Earth Planet. Inter. **120**, 43 (2000); Phys. Rev. B **59**, R14 141 (1999).
[39] D. L. Anderson, *Theory of the Earth* (Blackwell Scientific Publications, Boston, 1989).
[40] P. Hohenberg and W. Kohn, Phys. Rev. **136**, B864 (1964); W. Kohn and L. J. Sham, *ibid.* **140**, A1133 (1965).
[41] Y. Wang and J. P. Perdew, Phys. Rev. B **44**, 13 298 (1991).
[42] J. P. Perdew, S. Kurth, A. Zupan, and P. Blaha, Phys. Rev. Lett. **82**, 2544 (1999); S. Kurth, J. P. Perdew, and P. Blaha, Int. J. Quantum Chem. **75**, 889 (1999).
[43] G. Kresse and J. Furthmüller, Comput. Mater. Sci. **6**, 15 (1996); Phys. Rev. B **54**, 11 169 (1996).
[44] P. E. Blöchl, Phys. Rev. B **50**, 17 953 (1994); G. Kresse and D. Joubert, *ibid.* **59**, 1758 (1999).
[45] D. Vanderbilt, Phys. Rev. B **41**, 7892 (1990).
[46] S. G. Louie, S. Froyen, and M. L. Cohen, Phys. Rev. B **26**, 1738 (1982).
[47] A. M. Rappe, K. M. Rabe, E. Kaxiras, and J. D. Joannopoulos, Phys. Rev. B **41**, 1227 (1990).
[48] H. J. Monkhorst and J. D. Pack, Phys. Rev. B **13**, 5188 (1976).
[49] S. Nosé, Mol. Phys. **52**, 255 (1984). Equilibrium is easier with the Andersen thermostat [see D. Frenkel and B. Smit, *Understanding Molecular Simulation: From Algorithms to Applications* (Academic, San Diego, 2002)]. We checked that these two methods give practically identical thermal pressure.
[50] P. Vinet, J. Ferrante, J. R. Smith, and J. H. Rose, J. Phys. C **19**, L467 (1986).
[51] P. Vinet, J. H. Rose, J. Ferrante, and J. R. Smith, J. Phys.: Condens. Matter **1**, 1941 (1989).
[52] J. Hama and K. Suito, J. Phys.: Condens. Matter **8**, 67 (1996).
[53] R. E. Cohen, O. Gulseren, and R. J. Hemley, Am. Mineral. **85**, 338 (2000).
[54] At ultrahigh compressions, the Vinet and most other equations of state break down, as they do not have the limiting electron-gas behavior (Ref. 52). Also note, partly in connection with this comment, recent criticism of the Vinet EOS by Holzapfel (W. B. Holzapfel, Z. Kristallogr. **216**, 473 (2001)], who proposed his own equations of state satisfying the electron-gas limit.
[55] J.-P. Poirier and A. Tarantola, Phys. Earth Planet. Inter. **109**, 1 (1998).
[56] A. R. Oganov and J. P. Brodholt, Phys. Chem. Miner. **27**, 430 (2000).
[57] A. R. Oganov, J. P. Brodhot, and G. D. Price, Earth Planet. Sci. Lett. **184**, 555 (2001).
[58] J.-P. Poirier, *Introduction to the Physics of the Earth's Interior* (Cambridge University Press, Cambridge, 2000).
[59] R. J. Angel, in *Rev. Miner. Geochem.*, edited by R. M. Hazen and R. T. Downs (Mineralogical Society of America, Washington, 2001), Vol. 41, pp. 35–59; http://www.crystal.vt.edu/crystal/software.html
[60] However, in the Earth's mantle MgO is likely to contain at least 10 mol % FeO, the effect of which on elasticity at high pressures and temperatures is unknown and could be large.
[61] L. D. Landau and E. M. Lifshitz, *Course of Theoretical Physics*, Statistical Physics, Part I (Butterworth & Heinemann, Oxford, 1980), Vol. 5.
[62] V. N. Zharkov and V. A. Kalinin, *Equations of State of Solids at High Pressures and Temperatures* (Consultants Bureau, New York, 1971).
[63] P. Gillet, J. Matas, F. Guyot, and Y. Ricard, in *Microscopic Properties and Processes in Minerals*, Vol. 543, *NATO Science Series C*, edited by K. Wright and R. Catlow (Kluwer, Dordrecht, 1999).
[64] However, even for relatively small systems, the difference between $3N$ and $(3N-3)$ is small. For our supercell with 64 atoms this difference is just 1.6%.
[65] L. V. Al'tshuler, S. E. Brusnikin, and E. A. Kuzmenkov, Zh. Prikl. Mekh. Tekh. Phys. **161**, 134 (1987).
[66] V. S. Vorobev, High Temp. **34**, 391 (1996).
[67] We treat γ_∞ as a fitted parameter. In the limit of infinite compression, all matter behaves like a free-electron gas, for which the Grüneisen parameter is known to be $\frac{2}{3}$ (Ref. 65); however, the relevance of this result to nonmetals is unclear: nonmetallic compounds must undergo a phase transition to a metallic state before the limit $V/V_0=0$ is approached and it may be only the metallic phase to which the limit $\gamma_\infty=2/3$ is applicable. Nevertheless, a fit to our PAW results gives a value similar to $\frac{2}{3}$ ($\gamma_\infty=0.75$).
[68] Fitting these parameters to experimental data, we found that the resulting values of the parameters strongly depend on the weights given to different experimental data; parameters discussed here as ''experimental'' correspond to one particular set of results.
[69] O. L. Anderson, *Equations of State of Solids for Geophysics and Ceramic Science* (Oxford University Press, Oxford, 1995).
[70] D. G. Isaak, O. L. Anderson, and T. Goto, Phys. Chem. Miner. **16**, 704 (1989).
[71] M. W. Chase, Jr., NIST-JANAF Thermochemical Tables, J. Phys. Chem. Ref. Data Monograph, No. 9 (Am. Chem. Soc., Am. Inst. Phys., Nat. Inst. Stand. Tech., 1998).
[72] A. R. Oganov, J. P. Brodholt, and G. D. Price, Nature (London) **411**, 934 (2001); B. B. Karki, R. M. Wentzcovitch, S. de Gironcoli, and S. Baroni, Phys. Rev. B **62**, 14 750 (2000); Geophys. Res. Lett. **28**, 2699 (2001).